

Coarsening fronts

Arnd Scheel
University of Minnesota
School of Mathematics
206 Church St. S.E.
Minneapolis, MN 55455, USA

Abstract

We characterize the spatial spreading of the coarsening process in the Allen-Cahn equation in terms of the propagation of a nonlinear modulated front. Unstable periodic patterns of the Allen-Cahn equation are invaded by a front, propagating in an oscillatory fashion, and leaving behind the homogeneous, stable equilibrium. During one cycle of the oscillatory propagation, two layers of the periodic pattern are annihilated. Galerkin approximations and Conley index for ill-posed spatial dynamics are used to show existence of modulated fronts for all parameter values. In the limit of small amplitude patterns or large wave speeds, we establish uniqueness and asymptotic stability of the modulated fronts. We show that the minimal speed of propagation can be characterized by a dichotomy depending on the existence of pulled fronts. Main tools here are an Evans function type construction for the infinite-dimensional ill-posed dynamics and an analysis of the complex dispersion relation based on Sturm-Liouville theory.

Running head: Coarsening fronts

Corresponding author: Arnd Scheel, scheel@math.umn.edu

Keywords: Allen-Cahn, Chafee-Infante, coarsening, modulated fronts

1 The Allen-Cahn equation and coarsening

The Allen-Cahn equation We consider

$$u_t = u_{xx} + f(u), \quad x \in \mathbb{R}, \quad (1.1)$$

with $f(u) = u(1 - u^2)$, and initial condition $u(0, x) = u_0(x) \in BC^0(\mathbb{R})$, the bounded uniformly continuous functions on the real line. Recall that (1.1) is formally a gradient system in L^2 with respect to the energy

$$V(u) = \int_{\mathbb{R}} \left(\frac{1}{2} u_x^2 + F(u) \right) dx, \quad (1.2)$$

where $F(s) = \int_0^s f(s)$. In particular,

$$\frac{d}{dt} V(u(t, \cdot)) \leq 0,$$

for all solutions of (1.1) with $V(u_0(\cdot)) < \infty$.

We may also consider (1.1) with periodic initial conditions $u_0(x) = u_0(x + \frac{2\pi}{k})$ and recover

$$V_{\text{per}}(u) = \int_0^{2\pi/k} \left(\frac{1}{2} u_x^2 + F(u) \right) dx,$$

as a nonincreasing energy.

Layers and interaction In both cases, the solutions $u(t, x) \equiv 1$ and $u(t, x) \equiv -1$ are asymptotically stable equilibria. In the case of periodic boundary conditions, almost every trajectory converges to either one of the two equilibria. On the unbounded real line this is not true anymore: The families of translates of the stationary layer solutions

$$u_1^\pm(x) = \pm \tanh(x/\sqrt{2}), \quad (1.3)$$

are asymptotically stable with asymptotic phase

$$\|u(t, x) - u_1^\pm(x + x_0)\|_{BC^0} \rightarrow 0 \text{ for } t \rightarrow \infty,$$

for some small x_0 , if $\|u(0, x) - u_1^\pm(x)\| < \varepsilon$, small enough.

Even with periodic boundary conditions, layers can determine the actual dynamics on very large time scales. An initial condition consisting of alternating up and down layers u_1^\pm at positions x_i , $0 \leq i < 2N$, retains its shape as long as the differences $x_{i+1} - x_i$ remain large. The evolution of the positions is governed approximately by

$$\dot{x}_i = G(x_{i+1} - x_i) - G(x_i - x_{i-1}), \quad i \bmod 2N \quad (1.4)$$

with $G(y) \sim e^{-\sqrt{2}y}$ exponentially small for large layer spacing [3, 12]. Eventually, the difference $x_i - x_{i+1}$ will become small for two adjacent layers, and the two layers collide and annihilate, reducing the effective ODE (1.4) to $2(N - 1)$ variables. One consequence of this scenario is that, for k small, the temporal convergence towards the spatially homogeneous equilibria $u \equiv \pm 1$ can be very slow.

Attractors A somewhat different view on the dynamics is provided by the description of the *attractor* of the Allen-Cahn equation with periodic boundary conditions. The attractor \mathcal{A}_{per} consists of all solutions $u(t, x)$ which are bounded for all times $t \in \mathbb{R}$. It is a compact set and consists of the equilibria and connecting orbits between equilibria. The following diagram depicts the set of equilibria and the connecting orbits, depending on the parameter k which fixes spatial periodicity. The analysis of the Allen-Cahn equation under this dynamical systems view point goes back to Chafee and Infante [4]; see [14] for more information on attractors and [10] for a recent overview of attractors in scalar reaction-diffusion equations.

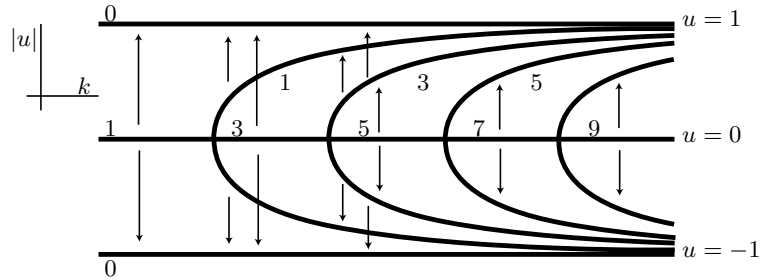


Figure 1.1: *Bifurcation diagram for the set of equilibria of the Allen-Cahn equation with parameter k . Nontrivial equilibria bifurcate from $u = 0$ at $k = 1, 2, \dots$ from left to right. The integers at branches denote the Morse indices. Only even representatives of nontrivial branches are shown. Arrows indicate connecting orbits between equilibria.*

For $k \rightarrow 0$, all branches of equilibria approach the layer-type configuration of solutions that we described above. Connecting orbits describe how perturbations of periodic layer configurations evolve into equilibria with fewer layers. For $k \notin \mathbb{Z}$, equilibria are hyperbolic up to a neutral eigenvalue induced by the spatial translation. We denote by i the number of unstable eigenvalues counted with multiplicity. The following result describes the set of connecting orbits. We denote by u_ℓ the equilibria that bifurcate from the trivial solution at $k = \ell$ and let \mathcal{U}_ℓ be the circle generated by the spatial translation of those equilibria in BC^0 . We also set $\mathcal{U}_0^\pm = u_0^\pm(x) \equiv \pm 1$ and $\mathcal{U}_\infty = u_\infty(x) \equiv 0$.

Theorem 1 (Structure of the attractor) *There exists a heteroclinic orbit from \mathcal{U}_ℓ to $\mathcal{U}_{\ell'}$ if, and only if $\ell > \ell'$, or, equivalently, if $i(u_\ell) > i(u_{\ell'})$.*

Note that, as a consequence, $V_{\text{per}}(u_\ell) > V_{\text{per}}(u_{\ell'})$ for $\ell > \ell'$.

Coarsening in space Our interest here is in the Allen-Cahn equation on the real line. The bifurcation diagram for equilibria gives a continuous family of periodic solutions $u_{\text{per}}(x; k)$, with $u_{\text{per}}(x; k) = u_{\text{per}}(x + \frac{2\pi}{k}; k)$, $0 < k < 1$. For $k \rightarrow 1$, $u_{\text{per}}(x; k) \rightarrow 0 =: u_{\text{per}}(x; 1)$. For $k \rightarrow 0$, the periodic solutions converge locally to a concatenation of up and down layers. All these periodic solutions are linearly and nonlinearly exponentially unstable. The question that motivates the present paper is how fast this instability spreads when initiated locally in space. There are two scenarios, where intuition provides a fairly complete picture. First, consider $k = 1$, that is, perturbations of the trivial homogeneous state. Positive perturbations with compact support can be shown to evolve into two fronts, marking the interface between the

stable state $u \equiv 1$ and the unstable state $u \equiv 0$ at $\pm\infty$. The spreading speed of these fronts is known to be $c = 2$. The fronts on both sides are solutions of the form $u(x - ct)$, which solve the traveling wave ODE

$$u_{\xi\xi} + cu_{\xi} + f(u) = 0, \quad u(\xi) \rightarrow 1 \text{ for } \xi \rightarrow -\infty, \quad u(\xi) \rightarrow 0 \text{ for } \xi \rightarrow \infty.$$

Another limiting case is $k \sim 0$, when the unstable periodic patterns consists of plateaus at ± 1 separated by layers. A positive perturbation in the region where $u \sim -1$ would cause the layers that bound this region to the left and to the right to approach and eventually annihilate each other, thus creating a large region where $u \sim +1$. In the next step, the layers that bound this large region would then approach their neighboring layers and merge with those (they are attracted by these neighboring layers according to (1.4) and this force is not balanced by a layer on the other side since this one was annihilated in the previous step), annihilating two more intervals where $u \sim -1$. It is not hard to envision how this process would repeat periodically.

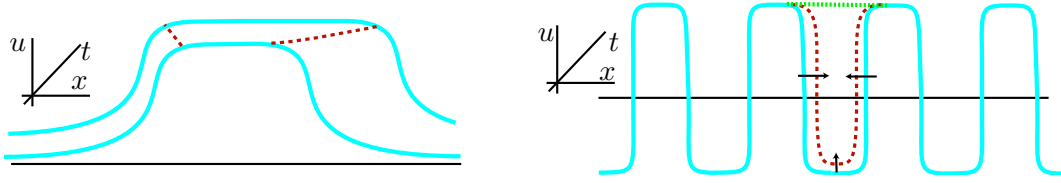


Figure 1.2: *Spreading of two fronts in the case $k = 1$ (left), and annihilation of layers in the case $k \sim 0$ (right).*

In both cases, the process is described by the superposition of two propagation mechanisms toward $\pm\infty$. The following definition captures these individual propagation mechanisms.

Definition 1.1 (Coarsening Fronts) *We call a solution $u(x, t)$ to (1.1) a coarsening front, if*

$$u(t, x) = u_{\text{cf}}(x - ct, kx), \quad u_{\text{cf}}(\xi, y) = u_{\text{cf}}(\xi, y + 2\pi),$$

and

$$\sup_y |u_{\text{cf}}(\xi, y) - u_{\text{per}}(y; k)| \rightarrow 0, \text{ for } \xi \rightarrow \infty \quad \sup_y |(u_{\text{cf}}(\xi, y))^2 - 1| \rightarrow 0, \text{ for } \xi \rightarrow -\infty.$$

A slight generalization of the definition would allow for a periodic pattern $u_{\text{per}}(y; k')$ at $-\infty$. Although our methods give existence results also for this more general type of fronts, we restrict to the somewhat simpler and more relevant case where $u_{\text{cf}} \rightarrow +1$ for the sake of simplicity.

The following theorems give some answers to the question of existence and uniqueness of coarsening fronts.

Theorem 2 (Existence) *Coarsening fronts exist for all $c > 0$ and all $0 < k \leq 1$.*

Theorem 3 (Uniqueness) *There is $c_u(k) \geq 0$ such that the coarsening fronts are unique for all $c > c_u(k)$, up to spatial and temporal translations. Moreover, $c_u(k) = 0$ for $k \sim 1$.*

The results also provide a partial answer to our question on the spreading speed of the instability: For suitable initial conditions, *any* speed of propagation of the stable state 1 into the unstable periodic state is possible.

The next interesting question is to which spreading speed is most likely to be observed. A stability analysis can give some insight into the size of the set of initial conditions which lead to propagation with a particular speed.

Again, the answer is somewhat discouraging. Define BC_η^0 as the set of continuous functions $u(x)$ with

$$\|u\|_\eta = \sup_{x \in \mathbb{R}} (1 + e^{\eta x}) |u(x)| < \infty. \quad (1.5)$$

The following theorem states that all fast fronts are stable and the speed of the slowest stable front is smooth in the limit of $k \sim 1$, when the asymptotic patterns are small.

Theorem 4 (Stability) *For each $0 < k \leq 1$ there is $0 < c_{\min}(k) < \infty$ such that all coarsening fronts are asymptotically stable for all $c > c_{\min}(k)$ in BC_η^0 for some suitable $\eta > 0$. For $c \lesssim c_{\min}(k)$, there exists an unstable coarsening front. Moreover, $c_{\min}(k) = 2 - 4(1 - k) + O((1 - k)^2)$ is smooth in $k = 1$, and the unique coarsening front is unstable if $c < c_{\min}(k)$ in this regime.*

We expect the results so far to be true for much more general invasion processes, possibly refining the notion of stability slightly. The stability result can be sharpened slightly when we exploit comparison principles. Consider the coarsening front $u_{\text{cf}}(x - ct, t)$ with the asymptotic periodic pattern $u_{\text{per}}(kx; k)$ in a frame moving with speed c , and linearize the evolution equation about these time-periodic solutions with period $T = 2\pi/(ck)$. The linearized equations are time-periodic parabolic equations

$$v_t = v_{\xi\xi} + cv_\xi + f'(u_{\text{cf}}(\xi, t))v, \quad (1.6)$$

with period map $v(T, \xi) = \Phi_{\text{cf}}^{c,k} v(0, \xi)$, and

$$v_t = \mathcal{L}_{\text{per}}^{c,k} v := v_{\xi\xi} + cv_\xi + f'(u_{\text{per}}(k(\xi + ct); k))v, \quad (1.7)$$

with period map $v(T, \xi) = \Phi_{\text{per}}^{c,k} v(0, \xi)$. We will see later that the spectral properties of these linear maps determine the nonlinear stability of the coarsening fronts.

Floquet theory [19] shows that $\rho = e^{\lambda T}$ is in the spectrum of Φ_{per} if and only if there exists an eigenfunction of the form

$$v(t, \xi) = e^{\lambda t} e^{\nu \xi} v_{\text{per}}(k(\xi + ct)), \quad (1.8)$$

where $v_{\text{per}}(y) = v_{\text{per}}(y + 2\pi)$ and $\nu \in i\mathbb{R}$. We then say λ belongs to the Floquet spectrum of Φ_{per} with Bloch wavenumber $\text{Im } \nu$. A short computation shows that v_{per} solves the eigenvalue problem in the steady frame

$$\tilde{\lambda} v = k(\partial_y + \nu)^2 v + f'(u_{\text{per}}(y))v, \quad \tilde{\lambda} = \lambda - c\nu. \quad (1.9)$$

Writing this ODE as a first order equation and evaluating the determinant $|\phi - \text{id}|$ with the corresponding period map ϕ , we find the *dispersion relation* $d(\tilde{\lambda}, \nu)$. In other words, λ belongs

to the essential Floquet spectrum if and only if $d(\lambda + c\nu, \nu) = 0$ for some $\nu \in i\mathbb{R}$. For each fixed ν , Sturm-Liouville theory asserts the existence of a sequence of eigenvalues $\lambda_k(\nu)$. In particular, $\lambda_0(\nu)$ corresponds to a positive eigenfunction, is simple, and $\operatorname{Re} \lambda_0(\nu) > \operatorname{Re} \lambda_j(\nu)$ for all ν and all $j > 0$.

For all λ in a compact part of the complex plane, there are only finitely many roots ν in any bounded part of the complex strip $\{0 \leq \operatorname{Im} \nu < k\}$, counting multiplicities. We label the roots (repeated by multiplicity) $\dots \operatorname{Re} \nu_{-2}(\lambda) \leq \operatorname{Re} \nu_{-1}(\lambda) \leq \operatorname{Re} \nu_0(\lambda) \leq \operatorname{Re} \nu_1(\lambda) \leq \operatorname{Re} \nu_2(\lambda) \leq \dots$, with labeling continuous unless $\operatorname{Re} \nu_j = \operatorname{Re} \nu_{j+1}$, when we possibly exchange labels, and with normalization $\operatorname{Re} \nu_{-1}(\lambda) < 0 < \operatorname{Re} \nu_0(\lambda)$ for $\lambda \gg 1$. We define the *absolute Floquet spectrum* Σ_{abs} as the set of λ such that $\operatorname{Re} \nu_{-1} = \operatorname{Re} \nu_0$; see [10, 18] for a more detailed description.

Definition 1.2 (Linear spreading speed) *We define the linear spreading speed as*

$$c_{\text{lin}}(k) = \inf\{c; \operatorname{Re} \Sigma_{\text{abs}}^{c,k} < 0\},$$

where Σ_{abs} denotes the absolute Floquet spectrum of the period map $\Phi_{\text{per}}^{c,k}$.

For the nonlinear equation, we use the “nonlinear eigenfunctions”, that is, periodic solutions to the nonlinear equation in a comoving frame, to define stability. It can be shown that with the choice of an exponential weight η according to $\operatorname{Re} \nu_{-1}(\lambda) < \eta < \operatorname{Re} \nu_0(\lambda)$, the linearized period map $\Phi_{\text{cf}} - e^{\lambda T}$ at a coarsening front is Fredholm of index zero for $\operatorname{Re} \lambda > -2$, that is, for λ to the right of the essential spectrum of the other asymptotic state $u \equiv 1$. We define the *extended Floquet point spectrum* Σ_{ext} as the set of λ for which the period map possesses a nontrivial kernel.

Definition 1.3 (Nonlinear spreading speed) *We define the nonlinear spreading speed $c_{\text{nl}}(k)$ as the infimum over all speeds c for which $\operatorname{Re} \Sigma_{\text{abs}}^{c,k} < 0$ and $\operatorname{Re} \Sigma_{\text{ext}}^{c,k} < 0$. In case of nonuniqueness, we require the second condition for all coarsening fronts.*

The following result summarizes and slightly sharpens the previous theorems in the terminology of linear versus nonlinear spreading speeds.

Theorem 5 *At the linear spreading speed, $\lambda = 0$ is the edge of the rightmost branch of absolute spectrum, with a positive eigenfunction: there is $\nu_0 > 0$ such that $\lambda_0(\nu_0) + c_{\text{lin}}\nu_0 = 0$, and $\lambda_0'(\nu_0) = c_{\text{lin}}$. If $c_{\text{nl}}(k) > c_{\text{lin}}(k)$, then $\lambda = 0$ belongs to the extended point spectrum with a positive eigenfunction for $c = c_{\text{nl}}(k)$. For $k \sim 1$, $c_{\text{lin}}(k) = c_{\text{nl}}(k) = 2 + 4(k - 1) + \mathcal{O}(k - 1)^2$. In particular, the invasion of patterns is slower than the invasion of the homogeneous state. For $k \sim 0$,*

$$c_{\text{lin}} = \frac{48\pi \sinh(p_*)}{k} e^{-\sqrt{2}\pi/k(1 + \mathcal{O}(e^{-\delta/k}))}, \quad \text{and } \nu/k \rightarrow p_*/\pi,$$

where $p_* = 1.54340\dots$ is the unique positive root of $\cosh(z) + 1 - z \sinh(z)$, and $\delta > 0$ is a small constant.

Summarizing, there are two possible instability mechanisms which characterize the minimal spreading speed, a linear and a nonlinear one. In the linear case, the instability of the asymptotic periodic state changes from convective to absolute when c passes the critical speed. In the nonlinear case, a zero eigenvalue destabilizes the front. The latter instability can be seen as an “orbit flip”, where the asymptotics of the coarsening front to the periodic pattern change from monotonically decreasing to monotonically increasing as the critical speed is passed. At the critical speed, the front possesses a steeper decay. The critical speed would be determined by the nonlinear shape of the front, and not the linearization at the leading edge. This type of fronts has been referred to as *pushed front*, as opposed to the *pulled front* which propagates with the linear spreading speed [23]. We shall adopt this terminology in the following. In order to illustrate both scenarios, we describe the more intuitive picture of fronts invading homogeneous states in the next section.

Figure 1.3 summarizes the main result in a two-parameter plot. Fronts exist in the entire parameter plane. The regime below c_{lin} contains only unstable fronts. Fronts in the upper part, large speed, and in the right part, $k \sim 1$ and $c \geq c_{\text{lin}}$ are stable. The curve c_{nl} bifurcating from c_{lin} illustrates the only possible instability mechanism which limits our results: Fronts would be stable above the curve c_{nl} , but unstable below. For values of k where c_{nl} differs from c_{lin} , pushed fronts with a steeper decay in the leading edge determine the mode of propagation. For $k \sim 1$, we showed that $c_{\text{lin}} = c_{\text{nl}}$, pushed fronts do not exist.

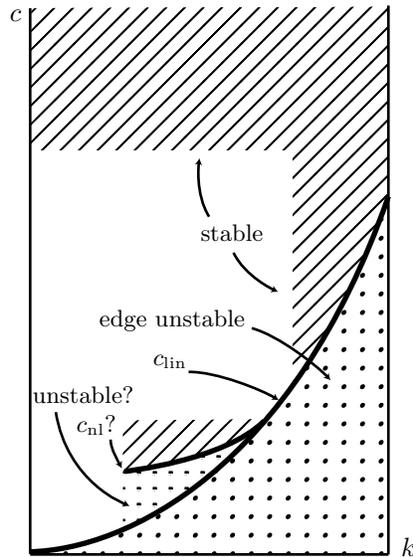


Figure 1.3: The figure shows the $c - k$ -parameter plane. Fronts exist for $0 < k \leq 1$. Fronts are unstable below c_{lin} . Fronts are stable in the upper part and in the right-hand part of the remaining area. The curve c_{nonlin} in the figure illustrates the only possible instability mechanism in the intermediate regime.

We conclude with the results of numerical computations of c_{lin} . We solved the boundary value problem for $d(\lambda, \nu)$ numerically using Matlab and followed $\lambda'(\nu) = c$, $\lambda(\nu) = 0$ from $\nu = 1$, $\lambda = 1$, and $c = 1$ for $k = 1$ to $k = 0.35$. The behavior appears to be linear for $k > 0.6$ with

a cross-over to exponential behavior for smaller k . The resulting exponential weight gives the exponential decay rate at the leading edge of the front with linear spreading speed. In particular, spreading is slow at double wavelength $c_{\text{lin}}(k = 0.5) = 0.0914$, but almost invisible at 2.5 times the critical wavelength $c_{\text{lin}} = 0.0126$ at $k = 0.4$. Also, the quotient ν/k , describing the exponential decay exponent per period of the underlying pattern converges to 0.4913 as predicted. We will see in the proof that the behavior of ν/k is quite universal.

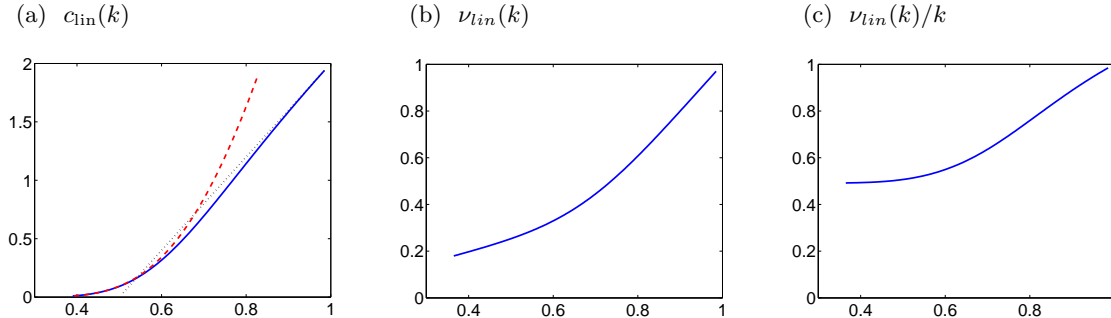


Figure 1.4: Numerically computed linear spreading speeds c_{lin} in comparison with theoretical prediction for $k \sim 1$ (dotted) and $k \sim 0$ (dashed), (a), and exponential decay rates, ν , at the edge as a function of the wave number k of the invaded pattern. The right figure (c) shows ν/k as a function of ν , which converge to $p_*/\pi \sim 0.4913$.

At $k = 0.37$, we found relative differences between the asymptotic expressions and the actual computation of c_{lin} and ν/k of the order 10^{-3} .

2 Front propagation — a short review

In this section, we illustrate the theorems in the simple case when $k = 1$ and $u_{\text{per}}(y) \equiv 1$. In order to exemplify the problems in the stability consideration, we consider the slightly more general nonlinearity $f(u) = u(1 - u^2) + \varepsilon u^2$, with $0 < \varepsilon$. The equation for modulated fronts can in this case be reduced by considering only y -independent solutions, which solve the traveling-wave equation

$$u_\xi = v, \quad v_\xi = -cv - f(u). \quad (2.1)$$

Elementary phase plane analysis shows existence of fronts connecting $u = 1$ to $u = 0$ for all $c > 0$, $\varepsilon = 0$. Close to $u = 0$, the fronts are monotone if $c^2/4 \geq f'(0) \geq 0$ or $c \geq 2$. For smaller values of c , the two eigenvalues of the linearization at $u = 0$ become complex.

The value of $c = 2$ is actually the linear spreading speed. The dispersion relation is

$$d(\tilde{\lambda}, \nu) = \tilde{\lambda} - \nu^2 + f'(0).$$

The absolute spectrum, where roots $\nu_{1,2}$ of $d(\lambda + c\nu, \nu)$ possess equal real part is given by

$$\Sigma_{\text{abs}} = \{\lambda < f'(0) - c^2/4\}.$$

In particular, $\lambda = 0$ lies at the edge of the absolute spectrum precisely for the linear spreading speed.

It is not difficult to see that the critical point spectrum in the space BC_η^0 coincides with the point spectrum in an L^2 -space with exponential weight $e^{-\eta\xi}$ for $\eta = c/2$. In this exponentially weighted space, the linearized operator

$$\mathcal{L}_{\text{tw}}w = w_{\xi\xi} + cw_\xi + f'(u_{\text{tw}}(\xi))w$$

becomes self-adjoint, conjugate to

$$\mathcal{L}_{\text{tw}}^{c/2}w = w_{\xi\xi} + [f'(u_{\text{tw}}(\xi)) - \frac{c^2}{4}]w,$$

with real spectrum.

For large c , singular perturbation theory shows that there are no unstable eigenvalues. Indeed, the linearized equation decouples into a trivial linear slow-fast system, excluding bounded solutions in the exponentially weighted norm.

We may then homotope in c and track zero eigenvalues. The crucial point is that eigenfunctions to the zero eigenvalue correspond to solutions of the linearized traveling-wave ODE. In particular, $\lambda = 0$ belongs to the spectrum if, and only if u_{tw} decays to zero with rate $e^{\nu_2\xi}$, where $|\nu_2| > |\nu_1|$, and the ν_j solve $\nu^2 + c\nu + f'(0) = 0$. As a consequence, fronts are stable if and only if they are monotonically decaying and positive.

In our case, $\varepsilon = 0$, this monotonicity property is a consequence of [1, 13]. For $\varepsilon > 1/\sqrt{2}$, there exists a unique front with the stronger exponential decay, explicitly given by $u_\xi = \frac{1}{\sqrt{2}}u^2 + \beta u$, $\beta^2 + c\beta = -1$, $\sqrt{2}\varepsilon + c + 3\beta = 0$, so

$$c = \frac{1}{2\sqrt{2}}(-\varepsilon + 3\sqrt{4 + \varepsilon^2}), \quad \beta = \frac{1}{2\sqrt{2}}(-\varepsilon - \sqrt{4 + \varepsilon^2}).$$

All fronts with speed $c < c_{\text{nl}}$ possess a single unstable real eigenvalue in the extended point spectrum and therefore in all exponentially weighted spaces that stabilize the essential spectrum, in particular in $BC_{c/2}^0$.

We summarize these gatherings in the following proposition.

Proposition 2.1 [13] *Suppose $\varepsilon \leq 1/\sqrt{2}$. Then $\text{Re } \Sigma_{\text{pt}}(L_{\text{tw}}) < 0$ for all $c \geq 2$. In particular, $c_{\text{lin}} = c_{\text{nl}}$.*

Suppose $\varepsilon > 1/\sqrt{2}$, next. Then $c_{\text{nl}} > c_{\text{lin}}$, that is $\text{Re } \Sigma_{\text{pt}}(L_{\text{tw}}) < 0$ for $c > c_{\text{nl}}$ and there is $0 < \lambda \in \Sigma_{\text{pt}}L_{\text{tw}}$ for $c < c_{\text{nl}}$.

Although there does not seem to be a rigorous proof in the literature, initial conditions with compact support actually approach two fronts with $c = \pm c_{\text{nl}}$, propagating towards $\pm\infty$.

Figure 2.1 summarizes these stability results in the $\varepsilon - c$ -parameter plane. Fronts exist in the entire parameter plane. The left boundary, $\varepsilon = 0$, coincides with the right boundary, $k = 1$, of Figure 1.3. The region below the curve c_{lin} contains fronts which are unstable due to an absolute instability at the leading edge. Fronts above c_{lin} but below c_{nl} are unstable due to a real unstable eigenvalue. The eigenfunction to this eigenvalue has a steeper decay than the

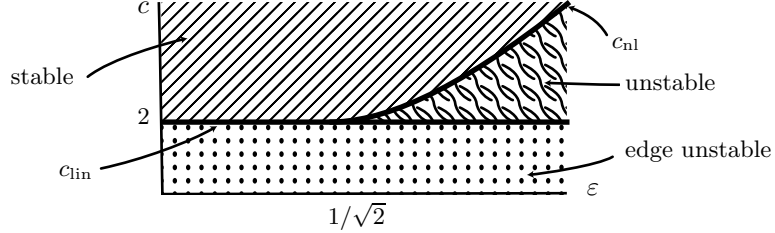


Figure 2.1: The figure shows the $\varepsilon - c$ -parameter plane. Fronts exist for all ε, c . Fronts are unstable below c_{lin} . Fronts are stable in the upper left part. Fronts are unstable below the curve c_{nl} , which bifurcates from $c_{\text{lin}} \equiv 2$ at $\varepsilon = 1/\sqrt{2}$.

front so that the instability manifests itself in a front splitting, where the steeper, pushed front with $c = c_{\text{nl}}$ is the one that is ultimately observed.

Intuitively, instability of fronts with $c_{\text{lin}} < c < c_{\text{nl}}$ can be understood as follows. For large ε , the origin $u = 0$ and the unique negative equilibrium are very close. In a rescaled version, they merge in a saddle-node bifurcation at $\varepsilon = \infty$. The linear instability of the origin therefore is very weak and the linear spreading speed quite small. On the other hand, there does exist a front connecting the positive stable state to the metastable negative state, with a speed of propagation bounded away from zero uniformly in ε large. Slow fronts connecting the positive stable state and the unstable zero state can therefore be overtaken by a faster mechanism, mimicking the competition between the stable and the metastable state.

Our results, $\varepsilon = 0$, $0 < k < 1$, parallel this ODE scenario, with the wavenumber k playing the role of the parameter ε . In particular, Figure 1.3 on existence and stability of modulated waves resembles the results on traveling waves, Figure 2.1. The main open question is to whether there is a curve c_{nl} bifurcating from c_{lin} in Figure 1.3. The intuitive reason for the existence of such a curve does not immediately carry over. However, for $k \sim 0$, the unstable periodic pattern does indeed resemble a metastable pattern of interacting layers, so that a pushed mode of propagation, different from the purely linear spread of the instability might well govern the spread of coarsening.

3 Modulated fronts

3.1 Modulated front equation and regularity

We look for coarsening front solutions of the Allen-Cahn equation according to Definition 1.1. Coarsening fronts solve a modulated traveling-wave equation

$$(\partial_\xi + k\partial_y)^2 u + c\partial_\xi u + f(u) = 0, \quad u(\xi, y) = u(\xi, y + 2\pi).$$

In analogy to the traveling-wave equation from Section 2, we consider this system as an—now ill-posed—dynamical system in the spatial ξ -variable. The idea of considering time-periodic parabolic problems on an unbounded domain as dynamical systems in the spatial direction goes back to [15], who built upon methods introduced by Kirchgässner [16] to find small

solutions via center-manifold reduction. Our approach here is closer to [11] since we need to consider solutions of not necessarily small amplitude.

We first rewrite the modulated traveling-wave equation as a first-order system in the ξ -variable.

$$\begin{aligned} u_\xi &= k\partial_y u + v \\ v_\xi &= k\partial_y v + \omega\partial_y u - cv - f(u). \end{aligned} \quad (3.1)$$

Coarsening fronts u need to satisfy certain boundary condition at $\xi = \pm\infty$,

$$\begin{aligned} (u, v)(\xi, \cdot) - (1, 0) &\rightarrow 0 \text{ for } \xi \rightarrow -\infty \\ (u, v)(\xi, \cdot) - (u_{\text{per}}(y), 0) &\rightarrow 0 \text{ for } \xi \rightarrow \infty. \end{aligned} \quad (3.2)$$

Solving (3.1) on $(\xi, y) \in \mathbb{R} \times S^1$ is equivalent to solving in corotating coordinates, replacing y by $\sigma = y + k\xi$. More, precisely, if we set $(u, v)(\xi, y) = (\tilde{u}, \tilde{v})(\xi, y + k\xi)$, we find

$$\begin{aligned} \tilde{u}_\xi &= \tilde{v} \\ \tilde{v}_\xi &= \omega\partial_\sigma \tilde{u} + c\tilde{v} - f(\tilde{u}). \end{aligned} \quad (3.3)$$

We consider (3.3) as an (ill-posed) evolution equation on $Y_p = H^{1/2,p}(S^1) \times L^p(S^1)$. The domain of the linear part of the right hand side as an unbounded operator on y is $Y_p^1 = H^{1,p}(S^1) \times H^{1/2,p}(S^1)$. Here, $H^{1,p}(S^1)$ and $H^{1/2,p}(S^1)$ are defined as the domains of the operators $|\partial_x|$ and $|\partial_x|^{1/2}$. We omit the index p whenever $p = 2$.

The linear equation

$$\begin{aligned} \tilde{u}_\xi &= \tilde{v} \\ \tilde{v}_\xi &= \omega\partial_\sigma \tilde{u} - c\tilde{v} + \tilde{u}, \end{aligned} \quad (3.4)$$

or, short, $\tilde{u}_\xi - A\tilde{u} = 0$, possesses an exponential dichotomy. In particular, the operator $\mathcal{A} = \frac{d}{d\xi} - A$ is invertible with

$$\mathcal{A}^{-1} : \mathcal{Y} = L^2(\mathbb{R}, Y_p) \rightarrow H^1(\mathbb{R}, Y_p) \cap L^2(\mathbb{R}, Y_p^1).$$

Similar results hold on scales of Sobolev spaces.

Lemma 3.1 (Local regularity) *Suppose $\tilde{u} \in L^2(I, Y_p)$ for some subinterval $I \subseteq \mathbb{R}$ is a solution of (3.3), that is $\tilde{u} \in H^1(I, Y_p) \cap L^2(I, Y_p^1)$ and (3.3) is satisfied. Then there is an I -independent constant C such that*

$$|\tilde{u}|_{H^1(I, Y_p) \cap L^2(I, Y_p^1)} \leq C|\tilde{u}|_{L^2(I, Y_p)}.$$

Proof. We first extend the solution with a smooth cut-off function to a function on $\xi \in \mathbb{R}$ which vanishes for large $x \notin I$. The extended function \tilde{u} satisfies

$$\tilde{u}_\xi = A\tilde{u} + h(\xi),$$

with $|h(\xi)|_{L^2(I, Y_p)} \leq \tilde{C}|\tilde{u}|_{L^2(I, Y_p)}$. We then use the resolvent estimate for A to conclude the proof of the lemma. \blacksquare

From the proof, it is clear that a simple bootstrap argument actually gives bounds in arbitrarily high Sobolev spaces. In particular, the uniform bounds carry over to uniform bounds in L^2 -based Sobolev spaces for (3.1).

A more tractable approximation to (3.3) is the Galerkin approximation

$$\begin{aligned}\tilde{u}_\xi &= \tilde{v} \\ \tilde{v}_\xi &= \omega \partial_\sigma \tilde{u} - c \tilde{v} - P_m f(\tilde{u}).\end{aligned}\tag{3.5}$$

Here, P_m is the L^2 -orthogonal projection onto the Fourier modes $e^{i\ell y}$, $|\ell| \leq m$. The projection P_m induces uniformly bounded projections on Y_p and Y_p^1 , which we denote by \mathcal{P}_m . The equation decouples into a skew-product on $\text{Im } \mathcal{P}_m$ and $\text{Im}(1 - \mathcal{P}_m)$,

$$\begin{aligned}\tilde{u}_\xi^0 &= A \tilde{u}^0 + \mathcal{P}_m F(\tilde{u}^0 + \tilde{u}^m), \\ \tilde{u}_\xi^m &= A \tilde{u}^m.\end{aligned}\tag{3.6}$$

Note that the second equation is explicitly solvable by Fourier decomposition. A trivial calculation shows that it does not possess any bounded solutions. The first equation is a $2m + 1$ -dimensional ODE. Note that the family of operators $\mathcal{P}_m F : Y_p \rightarrow Y_p$ is continuous in the space of smooth functions with respect to m at $m = \infty$, when restricted to an arbitrary fixed bounded subsets of Y , since $f(u)$ induces a compact operator from $H^{1/2,p}$ to L^p .

3.2 A priori estimates

We consider norms of solutions in the spaces $\mathcal{Y}_{p,a}$ and $\mathcal{Y}_{p,a}^1$, with norms

$$|u|_{\mathcal{Y}_{p,a}} := \sup_{\xi_0} \{|u(\cdot + \xi_0)|_{L^2((-1,1), Y_p)}\},$$

and

$$|u|_{\mathcal{Y}_{p,a}^1} := \sup_{\xi_0} \{|u(\cdot + \xi_0)|_{L^2((-1,1), Y_p^1)} + |u(\cdot + \xi_0)|_{H^1((-1,1), Y_p)}\}.$$

Again, we omit the index p when $p = 2$.

Definition 3.2 (Attractor) *We define the attractor $\mathcal{A}_m^{k,c}$ of (3.5) as*

$$\mathcal{A}_m^{k,c} = \{\tilde{u}(0, \cdot); \tilde{u}(\xi, \cdot), \xi \in \mathbb{R} \text{ is a solution to (3.5) and } |\tilde{u}|_{\mathcal{Y}_a} < \infty\}.$$

Whenever it is clear from the context, we will omit the superscripts c, k .

Proposition 3.3 *The union of the attractors is a compact set in Y . More precisely, there is $m_0 > 0$ such that*

$$\bigcup_{m_0 < m \leq \infty} \mathcal{A}_m \subset\subset Y$$

and bounded in Y^1 .

Proof. First notice that solutions in the attractors are smooth by local regularity.

Consider the function $H_4(\xi)$, defined through

$$H_4(\xi) := \frac{1}{4} \int_{S^1} u^3(\sigma)u(\sigma)d\sigma = \frac{1}{4}(u^3, u),$$

with (\cdot, \cdot) the scalar product in L^2 . The function H_4 is smooth in ξ and bounded on each solution in the attractor. We compute the derivatives

$$\frac{d}{d\xi}H(\xi) = (u^3, v),$$

and

$$\frac{d^2}{d\xi^2}H(\xi) = ((3u^2v, v) + (u^3, \omega u_\sigma) - (u^3, P_m f(u)) - c(u^3, v)).$$

The second term (u^3, u_σ) vanishes such that we find

$$H_{\xi\xi} - cH_\xi = ((3u^2)v, v) - (u^3, P_m f(u)).$$

The first term on the right hand side is positive and the second term can be rewritten

$$(u^3, P_m f(u)) = (u^3, u) - (P_m u^3, P_m u^3) = 4H(\xi) - |P_m u^3|_{L^2}^2.$$

Since $u = P_m u$,

$$\int u^4 = \int u^3 u = \int P_m u^3 P_m u \leq |P_m u^3|_{L^{4/3}} |u|_{L^4},$$

and we have

$$|P_m u^3|_{L^{4/3}} \geq |u|_{L^4}^3. \quad (3.7)$$

Now, by Hölder's inequality and (3.7)

$$|P_m u^3|_{L^2}^2 \geq c|P_m u^3|_{L^{4/3}}^2 \geq c|u|_{L^4}^6 = cH(\xi)^{3/2}.$$

Therefore,

$$H_{\xi\xi} - cH_\xi \geq -4H + cH^{3/2},$$

such that $H \leq 16/c^2$. This yields an a priori bound on $f(u)$ in $L^{4/3}$ and after a simple boot strap the desired a priori bounds. Indeed, we find that \underline{u} solves an equation

$$\underline{u}_\xi = A\underline{u} + h(\xi),$$

with $|h|_{Y_{p,a}} \leq M'$, with M' independent of m and the solution u with $p = 4/3$. This gives uniform bounds on $\underline{u}(\xi)$ and therefore the attractors in Y_p and Y_p^1 . By the embedding $Y_p^1 \rightarrow Y_\infty$, we have $|h|_{Y_{2,a}} \leq M'$ such that we can conclude the a priori bounds in Y and Y^1 .

It remains to show closedness. This can be easily established from convergence of subsequences of solutions $\underline{u}_\ell(\xi)$ in finite intervals $\xi \in (-\ell, \ell)$, after exploiting compactness of the closure and passing to a diagonal sequence. Regularity shows that the limiting function on $\xi \in \mathbb{R}$ is again a solution. \blacksquare

Proposition 3.4 *The map $\varphi_m(\xi) : \underline{u}(0) \mapsto \underline{u}(\xi)$ defines a flow on \mathcal{A}_m , which is continuous jointly in m and $\underline{u}(0)$.*

Proof. For $m < \infty$ solutions in the attractor are solutions to a smooth ODE and nothing needs to be proved. For $m = \infty$, the flow is well-defined since the Cauchy problem possesses unique solutions; see [5, 19]. Compactness together with uniqueness ensures continuity at $m = \infty$: suppose $\underline{u}_\ell(0) \rightarrow \underline{u}(0)$ but $\underline{u}_\ell(\xi) \not\rightarrow \underline{u}(\xi)$ for some ξ . Then, by compactness $\underline{u}_\ell(\xi) \rightarrow \tilde{\underline{u}}(\xi)$, which after extracting a diagonal sequence we may assume to be a solution in the attractor, passing through $\underline{u}(0)$, but different from the solution $\underline{u}(\xi)$, thus contradicting uniqueness. Continuity in m at $m = \infty$ states that the limits of the Galerkin approximation converge to (unique) solutions, which again is an easy consequence of compactness and uniqueness. ■

3.3 A Lyapunov function

Consider

$$V(u, v) = \frac{1}{2}(v, v) + k(v, u_\sigma) + (P_m F(u), 1), \quad (3.8)$$

Here, (\cdot, \cdot) again denotes the $L^2(0, 2\pi)$ -scalar product and $F(u) = \frac{1}{2}u^2 - \frac{1}{4}u^4$.

The function V is smooth on Y^1 , in particular on the attractors \mathcal{A}_m , and therefore is smooth as a function of ξ when (u, v) are solutions.

Proposition 3.5 *The function V is a strict Lyapunov function on \mathcal{A}_m , that is,*

$$\frac{d}{d\xi} V(u(\xi), v(\xi)) = -c|v + ku_\sigma|_{L^2}^2 \leq 0.$$

Proof. We compute

$$\begin{aligned} \frac{d}{d\xi} V &= (v, \omega u_\sigma - cv - P_m f) + k(\omega u_\sigma - cv - P_m f, u_\sigma) + k(v, v_\sigma) + (P_m f, v) \\ &= \omega(u_\sigma, v) - ck(u_\sigma, v) - c(v, v) + \omega k(u_\sigma, u_\sigma) \\ &= -c|v + ku_\sigma|^2 \leq 0, \end{aligned}$$

where we used $\omega k = c$, and $(P_m f, u_\sigma) = 0$, and $(v, v_\sigma) = 0$. ■

Note that on the set of relative equilibria, $v = -ku_\sigma$, V coincides with the *negative* energy for the parabolic flow,

$$V(u, -ku_\sigma) = -\left[\frac{1}{2}(u_\sigma, u_\sigma) - (P_m F(u), 1)\right].$$

We denote by \mathcal{E}_m the set of relative equilibria, where $v \equiv -ku_\sigma$, that is, $u_\xi + ku_\sigma = 0$ or $u = u(\sigma - k\xi) = u(y)$, independent of time t in the steady frame.

Corollary 3.6 *Solutions in the attractor are (relative) equilibria or heteroclinic orbits for m sufficiently large. More precisely, let $\underline{u} \in \mathcal{A}_m$. Then either $\underline{u} \in \mathcal{E}_m$, or $\text{dist}(\underline{u}(\xi), \underline{u}_\pm(\cdot)) \rightarrow 0$ for some orbit $\underline{u}_\pm(\cdot) \in \mathcal{E}_m$.*

Proof. Since V is constant on the connected ω -limit set, we conclude that $V_\xi = 0$ and the ω -limit set consists of a single equilibrium (actually a single circle). Here, we use that the set of equilibria consists of a finite number of circles, a fact that we shall prove in Section 4.1, below. \blacksquare

For finite m , solutions still converge to the set of equilibria \mathcal{E}_m , but not necessarily towards a single equilibrium.

4 Existence of modulated fronts for all $c > 0$

4.1 Equilibria and bifurcation diagram

In order to establish existence of heteroclinic orbits, we start by analyzing the set of equilibria \mathcal{E} . As already pointed out, equilibria are precisely the stationary periodic solutions $u(y)$. In particular, the bifurcation diagram is given by Figure 1.1. Since all bifurcations are nondegenerate, supercritical, any compact part of the bifurcation diagram is robust under the Galerkin approximation P_m . For finite m , we may actually compute the unstable dimension of the equilibria inside $\text{Im } \mathcal{P}_m$.

Definition 4.1 (Morse indices) *We define the Morse index i_M of a relative equilibrium as the number of Floquet exponents ν to the linearization, counted with multiplicity, which have $0 \leq \text{Im } \nu < k$ and $\text{Re } \nu > 0$. We define the relative Morse index $i = i_M - m$.*

Lemma 4.2 *The relative Morse indices are independent of m for m sufficiently large and coincide with the negative Morse indices for the parabolic flow $u_t = k^2 u_{yy} + f(u)$.*

Proof. Floquet exponents ν solve the characteristic boundary-value problem

$$\mathcal{M}(\nu)w = [(\nu + k\partial_y)^2 + c\nu + P_m f'(u_*(y))] w = 0, \quad w \in H_{\text{per}}^2(0, 2\pi). \quad (4.1)$$

For $u_*(y) \equiv a$, constant, the roots can be computed explicitly from

$$(\nu + ik\ell)^2 + c\nu + a = 0,$$

where ℓ denotes the subspace spanned by $e^{i\ell y}$, left invariant by the linearization. We denote the two solutions in this subspace by ν_ℓ^\pm . In the case of $a = -2$, the equilibria $u \equiv \pm 1$, all ν_ℓ^\pm have opposite real part, such that $i = 0$. In the case $a = 1$, all roots ν_ℓ^\pm with $|\ell| \geq 1$ have opposite real parts, and $\nu_0^\pm < 0$, such that $i = 1$.

This proves the lemma for $k = 1$. The conclusion of the lemma for $k \geq 1$ follows from the bifurcation diagram if we can prove that the multiplicity of the zero eigenvalue coincides with the multiplicity in the parabolic problem since imaginary eigenvalues are excluded by the variational structure.

First note, that computing the kernel of $\mathcal{M}(0)$ is equivalent to computing the kernel of the parabolic problem. Therefore, geometric multiplicities coincide for $\nu = 0$. In order to compute

algebraic multiplicities, let w_0 belong to the kernel. A generalized eigenvector has to solve $\mathcal{M}(0)w_1 = \mathcal{M}'(0)w_0$, or

$$k^2 w_1'' + P_m f' w_1 = 2k w_0' - c w_0.$$

However the right-hand side does not belong to the image of the left-hand side, since the scalar product with the element of the kernel w_0 gives $c|w_0|_{L^2}^2 \neq 0$. Therefore, algebraic and geometric multiplicities coincide, and we have proved the proposition. ■

4.2 Modulated waves for the Galerkin approximation

For finite m , the modulated wave equation can be viewed as a gradient-like ODE. The following theorem gives complete information about the connecting orbit structure in the attractor.

Theorem 6 *Fix $k_{\min} > 0$. Then there exists $m_0 = m_0(k_{\min}) < \infty$ such that for all $m > m_0$ and for all equilibria u_{\pm} there exists a heteroclinic orbit of (3.5) connecting u_+ to u_- provided $i(u_-) > i(u_+)$.*

Proof. We use the Conley index to establish the existence of heteroclinic orbits between any two given equilibria; see [6, 9, 11]. Since all Morse indices coincide with the Morse indices of the parabolic problem up to a constant shift (and flow reversal), the attractor in the modulated wave-equation is, on the level of Conley homology, an m -dimensional unstable suspension of the attractor in the parabolic Allen-Cahn problem with periodic boundary condition. Existence of heteroclinic orbits there is a consequence of S^1 -equivariance and reflection $u \mapsto -u$, both of which are present in the modulated traveling wave equation as well; see [9] for more details on the connection graph in the Allen-Cahn equation. The fact that we consider periodic instead of Neumann boundary conditions, here, does not alter the connection graph, since isolating blocks and exit sets can be constructed as direct products over the action of the circle group and the Conley index, as the homotopy type of the quotient, is the same as in the case of Neumann boundary conditions with half the period. This shows existence of heteroclinic orbits as claimed. ■

4.3 Modulated waves for the full problem

In this section, we conclude the proof of Theorem 2. We fix a periodic pattern $u_-(y)$ with period $2\pi/k$, and we fix a wave-speed $c > 0$. We set $\omega = ck$ and consider the modulated traveling-wave equation with these parameters. Since the periodic pattern has minimal period with the given parameters, the Morse index is precisely 1. In particular, for each m , there exists a heteroclinic orbit $\underline{u}_m(\xi)$ connecting the periodic pattern with $u_+ = 1$. Also, note that for all m sufficiently large, there are no other equilibria u_* with values of the Lyapunov function between u_+ and u_- .

By compactness of the attractors we can assume that $\underline{u}_m(\xi)$ converges in $L_a^2((-M, M), Y)$ for any $M > 0$. By local regularity, this implies that the limiting function $\underline{u}(\xi)$ is a trajectory

in \mathcal{A} . By continuity of the Lyapunov function, the values of V span the interval between the values of V on u_- and u_+ . Therefore, the limiting function does not belong to the set of equilibria. The only other possibility is a heteroclinic orbit, which then has to connect u_+ and u_- as claimed, since there are no other equilibria with values of the Lyapunov function between u_+ and u_- .

Remark 4.3 *We emphasize that our connecting orbit picture in the Galerkin approximation is much more complete. We suspect that one can prove the existence of all the connections from the Galerkin approximation in the full problem by suitably defining a (renormalized) Floer-type homology for the full problem.*

5 Fast waves

We consider the modulated traveling-wave equation in a corotating frame (3.1)

$$\begin{aligned} u_\xi &= k\partial_y u + v \\ v_\xi &= k\partial_y v + \omega\partial_y u + cv - f(u), \end{aligned} \quad (5.1)$$

with $c = \omega/k = 1/\varepsilon$ large, and $k = O(1)$. Note that, for convenience, we reversed the sign of c , here. In an abstract notation, this reads

$$\underline{u}_\xi = \mathcal{A}\underline{u} + \tilde{f}(\underline{u}), \quad \mathcal{A} = \begin{pmatrix} k\partial_y & \text{id} \\ \omega\partial_y + 1 & k\partial_y + c \end{pmatrix}, \quad \tilde{f} = \begin{pmatrix} 0 \\ f - 1 \end{pmatrix}. \quad (5.2)$$

We consider this equation as an evolution equation on $D(\mathcal{A}) = Y^2 = H^{3/2}(S^1) \times H^{1/2}(S^1) \subset Y$.

Corollary 5.1 *The attractor of (5.2), defined as the initial values \underline{u} of bounded solutions $\underline{u}(\xi)$, is closed in Y^2 and compact in Y .*

On a formal level, we may easily pass to a slow limit in (5.1): the second equation, with $\omega = ck$ and $c = 1/\varepsilon$, gives a compatibility condition $v = -k\partial_y u + \varepsilon(f(u) - k\partial_y v)$, and therefore,

$$v = -k\partial_y u + \varepsilon(f(u) + k^2\partial_{yy}u) + O(\varepsilon^2).$$

Substituting this result into the first equation gives

$$u_\xi = \varepsilon(k^2\partial_{\sigma\sigma}u + f(u)), \quad (5.3)$$

up to order ε^2 . We rescale $\zeta = \varepsilon\xi$ and let Φ_ζ^0 denote the flow to the formal limiting equation.

The formal analysis above suggests rescaling space ξ also in (5.1),

$$\begin{aligned} u_\zeta &= \frac{1}{\varepsilon}(k\partial_y u + v) \\ v_\zeta &= \frac{1}{\varepsilon}(k\partial_y v - f(u) + \frac{1}{\varepsilon^2}(k\partial_y u + v)), \end{aligned} \quad (5.4)$$

or, in the abstract setting,

$$\underline{u}_\zeta = \frac{1}{\varepsilon}(\mathcal{A}\underline{u} + \tilde{f}(\underline{u})). \quad (5.5)$$

The following theorem makes the formal computation above rigorous in the sense of geometric singular perturbation theory; [8, 22, 2].

Theorem 7 *There exists a smooth function $\Psi : H^{3/2} \times (0, \varepsilon_0) \rightarrow H^{1/2}$ such that the graph $\mathcal{M} = \{v = \Psi(u; \varepsilon), |u| \leq R\}$ is an inertial manifold for the dynamics of (5.2). More precisely,*

- \mathcal{M} is maximal: every bounded solution of (5.2) with $\xi \in \mathbb{R}^+$ is contained in \mathcal{M} ; in particular, \mathcal{M} contains the attractor;
- there is a local flow Φ_ζ on \mathcal{M} whose trajectories solve (5.2);
- \mathcal{M} and the flow Φ are smooth in $\varepsilon > 0$.
- $|\Phi_1^\varepsilon(\cdot) - \Phi_1^0(\cdot)|_C^1 \rightarrow 0$ for $\varepsilon \rightarrow 0$, uniformly in $|\underline{u}| \leq R$.

Proof. The proof closely follows [22], and we restrict here to pointing out the necessary modifications. We start with a change of coordinates that diagonalizes the linear part \mathcal{A} . We therefore note that \mathcal{A} leaves the Fourier subspaces spanned by $e^{i\ell\sigma}$ invariant, and define the change of coordinates in each of these subspaces separately. Therefore set

$$\begin{aligned} \Lambda_\pm^\ell &= ik\ell + \frac{1}{2\varepsilon}(1 \pm \sqrt{1 + 4ik\ell\varepsilon}), \\ L^\ell &= -k^2\ell^2, \\ B^\ell &= \sqrt{1 + 4ik\ell\varepsilon}. \end{aligned} \quad (5.6)$$

The above equations define closed operators Λ_\pm and B on L^2 . We now introduce the new variables w_\pm via

$$w_\pm = \varepsilon B^{-1}(v - \Lambda_\mp u), \quad w_+ + w_- = u, \quad \Lambda_+ w_+ + \Lambda_- w_- = v. \quad (5.7)$$

The change of coordinates is a bounded operator from $(u, v) \in H^{1/2} \times L^2$ into $H^{1/2} \times H^{1/2}$. In the new coordinates, the equation becomes

$$\frac{d}{d\zeta} w_\pm = \frac{1}{\varepsilon} \Lambda_\pm w_\pm \pm B^{-1} f(w_+ + w_-). \quad (5.8)$$

Solutions which are bounded in forward time $\zeta > 0$ satisfy the following mild formulation

$$\begin{aligned} w_-(\zeta) &= e^{\Lambda_-\zeta/\varepsilon} w_-^0 + \int_0^\zeta e^{\Lambda_-(\zeta-\zeta')/\varepsilon} B^{-1} f(w_+(\zeta') + w_-(\zeta')) d\zeta' \\ w_+(\zeta) &= \int_\infty^\zeta e^{\Lambda_+(\zeta-\zeta')/\varepsilon} B^{-1} f(w_+(\zeta') + w_-(\zeta')) d\zeta'. \end{aligned}$$

With the elementary representation in the Fourier spaces, we can obtain estimates

$$\begin{aligned} |e^{\Lambda_-\zeta/\varepsilon}| &\leq C_-, \quad \zeta > 0 \\ |e^{\Lambda_+\zeta/\varepsilon}| &\leq C_+ e^{\zeta/\varepsilon^2}, \quad \zeta < 0, \end{aligned} \quad (5.9)$$

where norms are taken as operator norms on $H^{1/2}$ or L^2 , equivalently. We may cut off the nonlinearity outside of the attractor to achieve a global Lipschitz bound for f . Exploiting the spectral gap between Λ_- and Λ_+ , reflected in the estimates (5.9), a standard fixed point argument now shows the existence and smoothness of an invariant manifold with smooth flow. The manifold is given as a graph $w_+ = \psi(w_-)$ with $\psi = O(\varepsilon^2)$; see [22] for details in a very similar situation.

We address convergence of the flow on the manifold as $\varepsilon \rightarrow 0$, next.

Since $w_+ = O(\varepsilon^2)$, it is sufficient to compare the solutions to the two fixed point equations

$$w_-(\zeta) = e^{\Lambda_- \zeta / \varepsilon} w_-^0 + \int_0^\zeta e^{\Lambda_- (\zeta - \zeta') / \varepsilon} B^{-1} f((\text{id} + \psi)(w_-(\zeta'))) d\zeta',$$

and

$$u(\zeta) = e^{L\zeta} u^0 + \int_0^\zeta e^{L(\zeta - \zeta')} f(u(\zeta')) d\zeta',$$

where $L = k^2 \partial_{\sigma\sigma}$. The crucial estimates needed in the sequel are for the convergence of the semigroups. In the individual Fourier components, it is straightforward to obtain

$$\begin{aligned} |e^{\Lambda_+^\ell \zeta / \varepsilon} - e^{L^\ell \zeta}| &\leq C e^{-\sqrt{\ell}}, \\ |e^{\Lambda_+^\ell \zeta / \varepsilon} - e^{L^\ell \zeta}| &\leq C e^{-\sqrt{\ell}} |c\Lambda_+^\ell - L^\ell| |\zeta| \\ &\leq C e^{-\sqrt{\ell}} \min\{\ell^2, \varepsilon \ell^3\}. \end{aligned}$$

Interpolation then gives

$$|e^{\Lambda_+^\ell \zeta / \varepsilon} - e^{L^\ell \zeta}| \leq C e^{(-\sqrt{\ell} + \delta_1)\zeta} \varepsilon^{\delta_2} \zeta^{-\delta_3},$$

with δ_1, δ_3 arbitrarily small and $\delta_2 > 0$. The second main estimate is the convergence of B^{-1} to the identity, which we measure in combination with the smoothing of the semigroup:

$$|e^{L^\ell \zeta} (\text{id} - B_\ell^{-1})| \leq C e^{-\ell^2 \zeta} \varepsilon \ell.$$

Putting these estimates together, it is straightforward to conclude convergence of the fixed points at any fixed positive time $\zeta > 0$; see again [22] for more details in a similar setting. ■

From the convergence of the flows and a priori bounds on the attractors, we can conclude that the structurally stable heteroclinic orbits in the Chafe-Infante attractor persist for finite $\varepsilon > 0$. This shows uniqueness of the coarsening fronts for large speed c as claimed in the first part of Theorem 3.

6 Small amplitude patterns ahead $k \sim 1$

We study in somewhat closer detail the case of small amplitude patterns, in particular since it allows for the most comprehensive stability analysis.

Consider the equation

$$\begin{aligned} u_\xi &= v \\ v_\xi &= \omega \partial_\tau u - cv - f(u). \end{aligned} \tag{6.1}$$

Recall the action of the circle group S^1

$$T_\theta \underline{u}(\cdot) = \underline{u}(\cdot - \theta), \quad \underline{u}(\tau) = (u(\tau), v(\tau)),$$

which maps solutions of (6.1) into solutions.

The fixed point space to this group action consists of time τ -independent functions and the ξ -dynamics are given by the traveling-wave ODE

$$\begin{aligned} u_\xi &= v \\ v_\xi &= -cv - f(u), \end{aligned} \tag{6.2}$$

with unique heteroclinic orbits $\underline{u}(\xi) \rightarrow (0, 0)$ for $\xi \rightarrow \infty$ and $\underline{u}(\xi) \rightarrow (1, 0)$ for $\xi \rightarrow -\infty$, for all $c > 0$. For $c \geq 2$, the fronts are monotone $u'(\xi) < 0$, and

$$\begin{aligned} \lim_{\xi \rightarrow \infty} u(\xi) e^{-\nu \xi} &> 0, & \text{for } c > 2, \quad \nu &= \frac{1}{2}(-c + \sqrt{c^2 - 4}), \\ \lim_{\xi \rightarrow \infty} u(\xi) e^{\xi} &= \infty, & \text{for } c &= 2. \end{aligned}$$

In the next step, we study the vicinity of $u = v = 0$ and $u = 1, v = 0$ in the full phase space. The linearization at $u = 1$ is

$$u_\xi = v, \quad v_\xi = \omega \partial_\tau u - cv + 2u,$$

with eigenvalues solving $\nu^2 = \omega i \ell - c\nu + 2$, $\ell \in \mathbb{Z}$. In particular, all eigenvalues have nonzero real part for all $c \geq 0$, and we conclude that the relative Morse index is zero; see [19, 10] for the definition of the relative Fredholm index.

The analysis in the following has been outlined already in [20], and we repeat the main arguments here for the sake of completeness. The heteroclinic bifurcation picture in the full phase space is depicted in Figure 6.1. The eigenvalues of the linearization at the equilibrium $u = 0$ solve $\nu^2 = \omega i \ell - c\nu - 1$. In particular, $\nu = i\gamma$ is an eigenvalue if and only if $\gamma^2 = 1$ and $c\gamma = \omega \ell$. We choose $\omega \sim c$ and see that a simple pair of eigenvalues crosses the imaginary axis at $\omega = c$, in the $\ell = 1$ subspace. As ω crosses the (fixed) value $\omega = c$, a periodic orbit bifurcates towards $\omega < c$ (which corresponds to $k < 1$, the region of existence), which is unstable inside the local center-manifold (since a direct computation shows that the equilibrium is stable inside the center-manifold for $k < 1$). The relative Morse index of the origin is -1 for $k > 1$ and $+1$ for $k < 1$.

In a neighborhood of the heteroclinic orbit in $\text{Fix } S^1$, we can construct the unstable W^u manifold of $u = 1$ and the strong stable manifold of the origin $u = 0$, $W^{ss}(0)$. We claim that at the bifurcation, $W^u(1)$ intersects $W^{ss}(0)$ transversely. From the consideration of relative Morse indices, this claim is true if the derivative of the front solution is the only

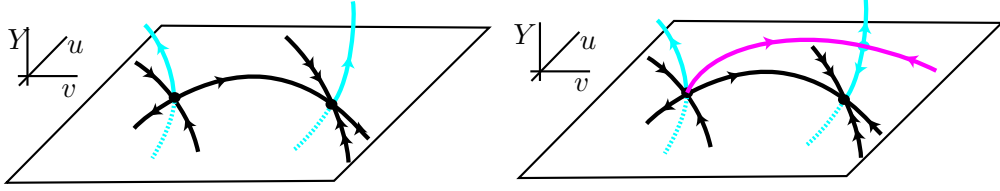


Figure 6.1: *Heteroclinic connection, stable, and unstable manifolds, before (left, $k > 1$) and after (right, $k < 1$) bifurcation. The ODE traveling-wave subspace is flow-invariant, horizontal. In the direction perpendicular to this subspace, the right equilibrium undergoes a Hopf bifurcation, here sketched as a pitchfork. The pink connection in the full space Y is the modulated wave for $k < 1$, bifurcating from the pure traveling wave, the black connection.*

bounded solution to the linearized equation. However, any solution to the linearized equation in a subspace $\ell \neq 0$ yields a purely imaginary eigenvalue to the linearization of the primary front solution in an L^2 -space with exponential weight $e^{-c\xi/2}$, which is impossible since the linearization at the primary front is self-adjoint in this weighted space.

Next, since the center-manifold is continuously fibered, the strong stable manifold of the bifurcating periodic orbit is close to the strong stable manifold of the origin in a smooth topology, and therefore intersects $W^u(1)$ transversely as well. The intersection between these two manifolds yields the desired coarsening front. Uniqueness follows from transversality and a priori bounds on the coarsening fronts.

7 Stability of coarsening fronts

In this section, we study stability of coarsening fronts. Since the asymptotic periodic pattern is always unstable, coarsening fronts are linearly (and nonlinearly) unstable in any uniform, translation-invariant norm. A standard way to overcome this problem and to single out a stable invasion process is to use exponential weights.

This section is organized as follows. We first recall the general framework for the study of spectral properties in Section 7.1. We then give some background on absolute and extended point spectra in Section 7.2. In Section 7.3, we characterize essential and absolute spectra at the periodic patterns in comoving frames and exponential weights. The results are used in Section 7.4 to prove the results on linear spreading speeds in Theorem 5. We then analyze extended point spectra for fast waves and for small amplitude pattern invasion in Sections 7.5 and 7.6. We conclude in Section 7.7 with the proof of the results on nonlinear spreading speeds from Theorem 5.

7.1 The eigenvalue problem

We are interested in the spectrum Σ of the period map $\tilde{\Phi}_T$ of the linearization at a coarsening front

$$u_t = u_{\xi\xi} + cu_{\xi} + f'(u_*(\xi, \omega t))u, \quad (7.1)$$

where $T = 2\pi/\omega$, and $\omega = ck$. We say ρ belongs to the essential spectrum Σ_{ess} if Φ_T is not Fredholm with index 0. We say ρ belongs to the point spectrum if Φ_T is Fredholm with index 0 but not invertible, $\Sigma_{\text{pt}} := \Sigma \setminus \Sigma_{\text{ess}}$. In [19], we showed that Fredholm properties can be characterized in terms of an appropriate spatial dynamics formulation. Consider therefore the Floquet Ansatz in the linearized modulated wave equation

$$\begin{aligned} u_\xi &= v \\ v_\xi &= \omega u_\tau - cv - f'(u_*)u + \lambda u, \end{aligned} \tag{7.2}$$

with u_* given by the coarsening front $u_* = u_{\text{cf}}(\xi, \omega t)$. We showed that $\Phi_T - e^{\lambda T}$ is Fredholm if and only if (7.2) possesses exponential dichotomies on both \mathbb{R}_+ and on \mathbb{R}_- , and $\Phi_T - e^{\lambda T}$ is invertible if and only if (7.2) possesses an exponential dichotomy on \mathbb{R} . Moreover, the Fredholm index is given by the difference of the relative Morse indices of the dichotomies: $i = i_- - i_+$, where the relative Morse indices can be computed as the Fredholm index of the projection of the unstable subspace of the dichotomy on the unstable subspace of a reference equation where $\lambda \gg 1$ with the reference projection. Since the existence of exponential dichotomies is determined by the asymptotic equations alone, that is, with u_* replaced by u_{per} or 1, respectively in (7.2), we recover a version of Weyl's theorem which asserts that the essential spectrum is determined by the asymptotic behavior of the potential. More specifically, the Fredholm index of $\Phi_T - e^{\lambda T}$ jumps on the Fredholm borders, where the asymptotic problems possess spatially bounded solutions; see also the review [10] for more background on Fredholm properties versus dichotomies.

7.2 Exponential weights, absolute spectra, and extended point spectra

Since $u \equiv 1$ is stable, all Fredholm borders associated with this state are in the left half plane and will not be relevant to us. Fredholm borders associated with the periodic solution $u_{\text{per}}(k(\xi - ct))$ correspond to purely imaginary Floquet exponents, that is, to solutions of (7.2), with $u_* = u_{\text{per}}(kx)$, of the form $e^{\nu\xi}u_0(\xi - ct)$, where u_0 is $2\pi/k$ -periodic in ξ and $\nu \in i\mathbb{R}$. Substituting this Ansatz into (7.2) and passing back to a steady frame shows that u_0 solves

$$(\lambda + c\nu)u_0 = \left(\frac{d}{dx} + \nu\right)^2 u_0 + f'(u_{\text{per}}(kx))u_0,$$

with periodic boundary conditions. Denote by Ψ_λ the period map to the first-order system

$$u' = v, \quad v' = (\tilde{\lambda} - f'(u_{\text{per}}(kx)))u,$$

and let

$$d_0(\tilde{\lambda}, \nu) = \det(\Psi_{\tilde{\lambda}} - e^{2\pi\nu/k}). \tag{7.3}$$

Then λ belongs to a Fredholm border if

$$0 = d_{\text{co}}(\lambda, \nu) := d_0(\lambda - c\nu, \nu).$$

We will exploit this relation of the spectral properties in steady and comoving frames further in Section 7.3, below.

Since all periodic patterns are unstable, $d(\lambda, i\gamma)$ vanishes for some $\gamma \in \mathbb{R}$ and $\operatorname{Re} \lambda > 0$, which implies unstable essential spectrum in the comoving frame from (7.3), $\lambda_{\text{co}}(i\gamma) = \lambda(i\gamma) + ci\gamma$. Still, fronts may be stable with respect to spatially localized perturbations. There are two concepts that serve to characterize this notion of “local” stability. First, one can try to choose exponential weights in an appropriate fashion so that the spectrum is “most” stabilized. Second, one might consider only finite but large domains (which would of course have to move with the front to make it a permanent structure). In [18], we showed that both concepts of stability are quite similar: spectra in bounded domains converge to a limiting spectrum. The absolute spectrum Σ_{abs} describes the continuous part of this limiting spectrum, and can at the same time be characterized by an “optimal” choice of exponential weights. The extended point spectrum Σ_{ext} is the discrete part of the limiting spectrum which is independent of the boundary conditions; again, see [18, 10] for more information.

In the following, we summarize the characterization of absolute and extended point spectra that we need for our purpose. In exponentially weighted spaces

$$|u|_{L^2_\eta}^2 = \int_0^\infty |u(\xi)|^2 + \int_{-\infty}^0 |e^{-\eta\xi} u(\xi)|^2,$$

Fredholm borders shift to $d(\lambda, \nu) = 0$ with $\operatorname{Re} \nu = \eta$. In spatial dynamics, this corresponds to an exponential dichotomy “relative” to the weight η , that is, a splitting into subspaces with decay stronger than $e^{(\eta-\delta)\xi}$ for increasing ξ and decay stronger than $e^{(\eta+\delta)\xi}$ in backward direction, for some positive δ . The main characterization in [18] (see also [19] and [10] for the case of a modulated wave equation) describes the absolute spectrum as the set of λ such that (7.2) does not possess an exponential dichotomy with relative Morse index zero relative to *any* weight η . In particular, outside of the absolute spectrum, the spatial Floquet exponents can be divided into two sets ν_j^+ and ν_j^- with $\operatorname{Re} \nu_j^- < \eta < \operatorname{Re} \nu_j^+$, where ν_j^\pm , $j \in \mathbb{N}$ and η depend on λ . For $\lambda \in \Sigma_{\text{abs}}$, $\operatorname{Re} \nu_0^- = \operatorname{Re} \nu_0^+$, and a splitting of the exponents by real parts is not possible (preserving the relative numbers in the two sets).

Extended point spectra can now be easily characterized. For $\lambda \notin \Sigma_{\text{abs}}$, there exists, by definition, an exponential dichotomy on \mathbb{R}_- and on \mathbb{R}_+ relative to η . We say that $\lambda \in \Sigma_{\text{ext}}$ if there does not exist an exponential dichotomy relative to the weight η on \mathbb{R} . It is not difficult to see that the characterization of the extended point spectrum does not depend on the weight η .

We therefore concentrate on the description of the absolute spectrum of the periodic patterns as a first, necessary stability criterion in the next section.

7.3 Linear spreading speeds — the absolute spectrum

7.3.1 The steady frame

Consider the linearization

$$w_t = w_{xx} + f'(u_{\text{per}}(kx; k))w = \mathcal{L}^{\text{per}} w, \tag{7.4}$$

at a periodic pattern $u_{\text{per}}(kx; k)$, $0 < k < 1$.

We define the Bloch wave conjugate operator

$$\mathcal{L}_\gamma^{\text{per}} w := (\partial_x + i\gamma)^2 w + f'(u_{\text{per}}(kx; k))w, \quad (7.5)$$

as a closed and densely defined operator on L^2 with $2\pi/k$ -periodic boundary conditions. The spectrum of \mathcal{L}^{per} can now be described by means of these conjugate operators [7, §XIII.16].

Proposition 7.1 *The spectrum of \mathcal{L}^{per} on $L^2(\mathbb{R})$ is given by the union of the spectra of $\mathcal{L}_\gamma^{\text{per}}$ on L_{per}^2 with $\gamma \in [0, k)$.*

A simple way to express the spectrum of \mathcal{L}^{per} is the ODE

$$u_x = v, \quad v_x = -f'(u_{\text{per}}(kx; k))u + \lambda u,$$

with period map Φ_λ . Define

$$d_0(\lambda, \nu) = \det(\Phi_\lambda - e^{2\pi\nu/k}),$$

such that $d_0(\lambda, \nu) = 0$ if and only if ν is a Floquet exponent of Φ_λ .

Corollary 7.2

$$\lambda \in \text{spec } \mathcal{L} \iff d_0(\lambda, i\gamma) = 0 \text{ for some } \gamma \in [0, k).$$

7.3.2 Comoving frames

We now consider the linearization in a frame moving with speed c ,

$$w_t = w_{\xi\xi} + cw_\xi + f'(u_{\text{per}}(\xi + ct; k))w.$$

The spectrum of the period map Ψ to this periodically forced linear parabolic spectrum is characterized in the following proposition.

Proposition 7.3 ([21]) *The Floquet multiplier $\rho = e^{2\pi\lambda/\omega}$ belongs to the spectrum of Ψ if, and only if $d(\lambda - ci\gamma, i\gamma) = 0$ for some $\gamma \in [0, k)$.*

7.3.3 Exponential weights

We may also consider the linearization in exponentially weighted spaces. The spectrum of L_{per} in spaces with exponential weight $e^{-\eta x}$ is given by the set of λ for which $d(\lambda, \eta + i\gamma) = 0$. For fixed η and $\gamma = 0$, the spectrum consists of a sequence of eigenvalues $\lambda_j(\eta)$, and again $\text{Re } \lambda_0(\eta) > \lambda_\ell(\eta)$ for all $\ell > 0$ and all η , with positive eigenfunction.

Lemma 7.4 *We have $\lambda_0''(\eta) \geq 0$ for all η . Moreover, $\lambda_0'(\nu) = 2\nu(1 + o(1))$ as $\nu \rightarrow \infty$, $\nu \in \mathbb{R}$.*

Proof. The curve $\lambda_0(\eta + i\gamma)$ gives the spectrum of the operator $(\partial_x + \eta)^2 + f'(u_{\text{per}}(kx; k))$ on $L^2(\mathbb{R})$. $\lambda'' < 0$ would imply that $\text{Re } \lambda_0(\eta + i\gamma) > \lambda_0(\eta)$. In particular, this would yield a non-positive leading eigenfunction for small rational γ on a multiple of the period $2\pi/k$, contradicting the uniqueness of the leading positive eigenfunction. It remains to establish the asymptotics. From the boundary-value problem for λ_0 , we find that

$$\lambda'(\nu) = 2\nu + (u_0'(x; \nu), u_0^*(x; \nu)),$$

where we refer to $u_0(\cdot, \nu)$ as the (positive) eigenfunction associated with $\lambda_0 \in \mathbb{R}$, u_0^* the eigenfunction for the L^2 -adjoint, and denote by (\cdot, \cdot) the scalar product in $L^2(0, 2\pi/k)$. Now $u_0^*(x; \nu) = u_0(-x, \nu)$, and it is therefore sufficient to give uniform H^1 -bounds on the first eigenfunction as $\nu \rightarrow \infty$. Multiplying the eigenvalue problem by u and integrating gives the straightforward estimate

$$|u_0'|^2 \leq (\nu^2 - \lambda + \sup |f'(x)|) |u_0|^2.$$

On the other hand, rescaling $y = \nu x$, we obtain

$$[(\partial_y + 1)^2 + \frac{1}{\nu^2} f'(y/\nu) - \frac{\lambda}{\nu^2}] u_0 = 0,$$

with $2\pi\nu/k$ -periodic boundary conditions. On the entire real line, the leading edge of the spectrum of this operator is given by the edge of the absolute spectrum located at $\lambda/\nu^2 = 1 + O(1/\nu^2)$, by treating f' as an L^∞ -bounded perturbation. Truncating to a finite domain of length L gives a leading edge eigenfunction at the edge with a correction $O(1/L^2)$, hence $\lambda_0/\nu^2 = 1 + O(1/\nu^2)$ [18]. Substituting this expression in the estimate for $|u'|^2$ gives the desired uniform H^1 -bound. \blacksquare

7.4 The absolute spectrum in a comoving frame

In the comoving frame, the essential spectrum is easily computed from Proposition 7.3. The location of the absolute spectrum, however, is a somewhat more subtle question. Since the dispersion relation in the comoving frame is given by $d(\lambda - c\nu, \nu)$, we have an “explicit” branch of eigenfunctions $\lambda_0^{\text{co}}(\nu) = \lambda_0(\nu) + c\nu$. Note that $(\lambda_0^{\text{co}})'(\nu) = 0$ precisely when $\lambda_0'(\nu) = -c$. By Lemma 7.4, there exists a curve $\nu = \nu_0(c) \in \mathbb{R}$, with $\nu'(c) \leq 0$ and $\nu(c) \sim -c/2$ as $c \rightarrow \infty$, such that $\lambda_0'(\nu_0(c)) = -c$ and $(\lambda_0^{\text{co}})'(\nu) = 0$.

Proposition 7.5 *The rightmost edge of the absolute spectrum in a frame moving with speed c is given by $\lambda_0^{\text{co}}(\nu_0(c)) = \lambda_0(\nu_0(c)) - c\nu_0(c)$. In particular, $\text{Re } \lambda_0^{\text{co}}(\nu) > \text{Re } \lambda$ for all $\lambda \neq \lambda_0^{\text{co}}(\nu)$ in the absolute spectrum. Moreover,*

$$\frac{d\lambda_0^{\text{co}}(\nu_0(c))}{dc} \leq 0 \text{ for all } c > 0, \quad \lambda_0^{\text{co}}(\nu_0(c)) \sim -c^2/4 + O(1) \text{ for } c \rightarrow \infty.$$

Proof. We first note that the absolute spectrum lies to the left of the edge since we can achieve this bound with the fixed exponential weight ν . We have to show that λ_0^{co} actually belongs to the absolute spectrum. First note that this is true at $c = 0$. If the index of the two eigenvalues ν_0 and ν_1 that collide to form the double root were to change while increasing

c , we would have a $d(\lambda + c(\nu + i\gamma), \nu + i\gamma) = 0$ for some $\gamma \neq 0$. This however would again yield leading non-monotone eigenfunctions in a periodic domain with a suitable multiple of the period and therefore contradict monotonicity of the parabolic evolution.

The formula for the derivative is an immediate consequence of the chain rule and the fact that $(\lambda_0^{co})' > 0$, $\nu_0 < 0$, and $\nu_0' \leq 0$ for $c > 0$. The asymptotics follow from the asymptotics for $\lambda_0(\nu)$. \blacksquare

Remark 7.6 *The function $\lambda_* = H(c)$ for the leading edge is the Legendre transform of the function $\lambda_0(\nu)$ of the leading eigenvalue. Indeed, we obtain $H(c)$ if we solve the double-root condition $-c = \lambda_0'(\nu)$ for $\nu = \nu(c)$ and substitute the result into $H(\nu) = \lambda(\nu) + c\nu$.*

It is an easy exercise to compute the expansion for c_{lin} near $k = 1$. The small pattern is given to leading order by $\sqrt{8(1-k)/3} \cos(x)$, which, after Lyapunov Schmidt reduction on the kernel leads to the dispersion relation

$$\nu^2 + (1 - 4(1 - k)) = \lambda + c\nu + O((1 - k)^2).$$

The condition $\lambda = 0$ and $\frac{d\lambda}{d\nu} = 0$ give $c = 2\nu$ and $\nu^2 = 1 + 4(k - 1)$, from which we find $c = 2\sqrt{1 + 4(k - 1)}$ and the expansion in Theorem 5.

In the limit of $k \sim 0$, we use [17, §6.1] for the expansion of the dispersion relation near the unstable eigenvalue. From (100) there, we find

$$\lambda(\nu) = -16(\cosh(\nu L) + 1)e^{-L/\sqrt{2}}(1 + O(e^{-\delta L}))\left(-\frac{3}{2}\right)$$

(note that the results in [17] are stated for purely imaginary νL but extend to a complex strip by analyticity). The condition on the spreading speed attained at a double root gives

$$c = -\lambda'(\nu) = 24L \sinh(\nu L)e^{-L/\sqrt{2}} + O(e^{-L/(\sqrt{2}+\delta)})$$

with $L = \pi/k$ so that the Legendre transform is given by

$$\lambda - c\nu = 48(\cosh(\nu L) + 1 - (\nu L) \sinh(\nu L))e^{-\sqrt{2}L} + O(e^{-L/(\sqrt{2}+\delta)}).$$

The roots are to leading order given by $\nu L = p_* + O(e^{-\delta L})$, with p_* the unique solution of $\cosh(p) + 1 = \sinh(p)$. Substituting this expansion into the expression for c gives the expansion for the spreading speed.

7.5 Stability of fast waves

We claim that for large wave speeds, there exists an exponential dichotomy relative to the weight $\eta = c/2$, for all $\text{Re } \lambda > -M$, $M > 0$ fixed, arbitrarily large. We therefore closely follow the arguments in Section 5, applied to the eigenvalue problem (7.2). After passing to a corotating coordinate system and performing the scaling, we are left with a bounded perturbation of the linear part, given by

$$\underline{u}_\xi = \mathcal{A}\underline{u}, \quad \mathcal{A} = \begin{pmatrix} k\partial_y & \text{id} \\ \omega\partial_y - \lambda + 1 & k\partial_y + c \end{pmatrix}. \quad (7.6)$$

A somewhat tedious but straight-forward analysis shows that all estimates from Section 5 are uniform in $\operatorname{Re} \lambda > -M$. This shows the existence of a smooth (linear) center-stable manifold for the nonautonomous, perturbed system, which is precisely the stable subspace of the dichotomy relative to the weight $c/2$. Since the construction is valid on $\xi \in \mathbb{R}$, we have a dichotomy on $\xi \in \mathbb{R}$ and we can therefore excluded both absolute and extended point spectrum. This proves stability for large wave speeds.

7.6 Stability for $k \sim 1$

We view the fronts for $k \sim 1$ as a small perturbation of the fronts with $k = 1$. In particular, the variation in the coefficients of the linear equation (7.2) is small when measured in the L^∞ -norm with respect to ξ . As a consequence, exponential dichotomies (relative to any chosen weight) are continuous in k . We are interested in values of $c > c_{\text{lin}}(k)$, just above the linear spreading speed, and we have to show that there exists exponential dichotomies with Morse index zero relative to some exponential weight η . Note that for $c > 2$ and k small, this is an immediate consequence of the stability of the traveling waves connecting zero and one and the robustness of dichotomies cited above. The difficulty is that, as c approaches 1, the size of the allowed perturbation $k - 1$ shrinks to zero in standard perturbation theory: an eigenvalue could pop out of the edge of the absolute spectrum and create an instability. The key idea of obtaining stability for all $c \gtrsim c_{\text{lin}}(k)$ and $k \gtrsim 1$ is to extend the subspaces smoothly into $k = 1, c = 2$: although we loose the exponential separation property in the limit, we will be able to show robustness under perturbations to $k > 1$.

We start by continuing the subspaces smoothly for the asymptotic equation. At $k = 1$ and $c = 2$, the dispersion relation $d(\lambda, \nu) = \nu^2 + c\nu + 1 - \lambda$ possesses a double root in $\lambda = 0, \nu = 1$, corresponding to a Jordan block. If we substitute $\lambda = \alpha^2$, we can continue the roots ν smoothly as functions $\nu(\alpha)$ through $\alpha = 0$. By construction via the period map of an ODE, d is a smooth function of $k \gtrsim 1$, and we can follow the double root $\lambda = 0, \nu = \nu_*$ smoothly in k , varying $c = c(k)$, the linear spreading speed. Since the eigenvalues depend smoothly on the parameters α, k , the eigenfunctions and associated subspaces and projections are smooth as well. At $k = 1$, the continuation of both, unstable and stable subspaces of the dichotomy relative to the weight $\eta = c/2 = 1$ are given by the eigenspace to $\nu = 1$.

The remaining step is to show that these subspaces can be continued smoothly for the equation with the nonlinear front substituted into the linearized equation, instead of simply the periodic pattern. First note that without loss of generality we may assume that the double eigenvalue is given by $\nu = 0$ instead of $\nu = 1$ by passing to an exponential weight. We then write the unstable subspace as the graph of a linear map h from E^u into E^s , the stable and unstable subspaces of the asymptotic problem. We next write the eigenvalue problem in an abstract form, decomposing the solution vector $(u, v) = w^u + w^s$, where $w^{u/s} \in E^{u/s}$. The equation then reads

$$\begin{aligned} w_\xi^u &= A^u(\xi)w^u + B_u^u(\xi)w^u + B_s^u(\xi)w^s \\ w_\xi^s &= A^s(\xi)w^s + B_u^s(\xi)w^s + B_s^s(\xi)w^s, \end{aligned}$$

where $|B(\xi)| \leq Ce^{\kappa\xi}$ for some $\kappa > 0$ as $\xi \rightarrow -\infty$, and we suppressed the dependence on parameters. The graph of h provides an unstable subspace for the evolution if it is invariant, that is, if

$$h_\xi = (A^s h - h A^u) + (B_u^s + B_s^s h - h B_u^u - h B_s^u h) =: \mathcal{L}h + \mathcal{K}(h).$$

Here, both \mathcal{L} and \mathcal{K} depend on time and parameters. The operator \mathcal{L} generates the forward evolution $\mathcal{H}(\xi, \zeta)$,

$$\mathcal{H}(\xi, \zeta)h(\zeta) = \Phi^s(\xi, \zeta)h(\zeta)\Phi^u(\zeta, \xi), \quad \xi \geq \zeta,$$

where $\Phi^{u/s}$ denote the evolution operators associated with the dichotomy of the unperturbed equation. As a consequence,

$$|\mathcal{H}(\xi, \zeta)| \leq Ce^{-\delta(\xi-\zeta)}, \quad \xi \geq \zeta,$$

with δ arbitrarily small for parameter values $k \sim 1$ and $c \sim 2$. Also

$$|\mathcal{K}| \leq Ce^{\kappa\xi}(1 + |h|^2).$$

We seek exponentially decaying, continuous solutions $h(\xi), \xi \leq -\xi_*$, with

$$|h|_\iota = \sup_\xi e^{-\iota\xi}|h(\xi)| < \infty,$$

as fixed point of the integral equation

$$h(\xi) = \int_{-\infty}^{\xi} \mathcal{H}(\xi, \zeta)\mathcal{K}(h(\zeta))d\zeta.$$

A straightforward computation shows that the right-hand side defines a contraction if $\kappa > \iota$, $\kappa > \delta$, and $\xi_* \gg 1$, since the Lipschitz constant scales as $e^{-(\kappa-\iota)\xi_*}$. The fixed point depends smoothly on the parameters and provides us with the unstable subspace for the full nonautonomous equation.

For $k = 1$, $c = 2$ the unstable subspace converges exponentially to the eigenspace so that solutions in the unstable subspace decay exponentially $u(\xi) \sim e^\xi$. Since the front in the ODE and therefore also its derivative contain terms of the form ξe^ξ [1], the derivative of the front does not lie in the unstable subspace. In particular, the intersection of stable and unstable subspaces is transverse and persists as such. This excludes extended point spectrum for $c \sim 2$ and $k \sim 1$.

7.7 Pulled versus pushed fronts

In order to proof Theorem 5, it remains to show that whenever $\Sigma_{\text{ext}} \cap i\mathbb{R} \neq \emptyset$, $\text{Re } \Sigma_{\text{ext}} \leq 0$, then $0 \in \Sigma_{\text{ext}} \cap i\mathbb{R}$ with a positive eigenfunction. After multiplying with the exponential weight, we have to consider the period map to a parabolic equation with time-periodic coefficients, which we denote by Ψ . We consider Ψ in the space of uniformly continuous functions BC^0 with the supremum norm. We denote by E^c the finite-dimensional generalized eigenspace associated with the spectrum of Ψ on $i\mathbb{R}$ and P^c the associated spectral projection. Furthermore, let C

be the (closed) positive cone in BC^0 , that is, $C = \{u \mid u \geq 0\}$. Choose any $u \in C$. From the spectral decomposition, we know that $(1 - P_c)\Psi^k u \rightarrow 0$. If we choose $u(x) = |e_0(x)|$, with $0 \neq e_0(x) \in E^c$, then $\Psi^k(u)(x) > \Psi^k(e_0)(x)$, and, in particular, $\Psi^k(u)$ does not converge to zero. As a consequence, there exists a subsequence $k_\ell \rightarrow \infty$ such that $\Psi^{k_\ell}(u)/|\Psi^{k_\ell}(u)| \rightarrow u_* \in E^c$, $|u_*| = 1$. In particular, $S := E^c \cap C \neq \{0\}$. Let $S_1 = S \cap \{|u| \leq 1\}$ and \mathcal{S}_1 be the convex hull of S_1 . Then \mathcal{S}_1 is compact and convex, and invariant under the map $\Psi_1(u) := \Psi(u)/|\Psi(u)|$. By Schauder's fixed point theorem, there exists a fixed point of $\Psi_1(u)$ in \mathcal{S}_1 , which provides us with the desired positive eigenfunction.

References

- [1] D. G. Aronson and H. F. Weinberger. *Nonlinear diffusion in population genetics, combustion, and nerve pulse propagation*. Partial differential equations and related topics (Program, Tulane Univ., New Orleans, La., 1974), pp. 5–49. Lecture Notes in Math., Vol. 446, Springer, Berlin, 1975.
- [2] A. Calsina, X. Mora, and J. Solá-Morales. *The dynamical approach to elliptic problems in cylindrical domains, and a study of their parabolic singular limit*. J. Differential Equations **102** (1993), 244–304.
- [3] J. Carr and R. Pego. *Invariant manifolds for metastable patterns in $u_t = \epsilon^2 u_{xx} - f(u)$* . Proc. Roy. Soc. Edinburgh Sect. A **116** (1990), 133–160.
- [4] N. Chafee and E.F. Infante. *A bifurcation problem for a nonlinear partial differential equation of parabolic type*. Applicable Anal. **4** (1974/75), 17–37.
- [5] v X.-Y. Chen. *A strong unique continuation theorem for parabolic equations*. Math. Ann. **311** (1998), 603–630.
- [6] C. Conley. *Isolated invariant sets and the Morse index*. *CBMS Regional Conference Series in Mathematics* **38**. American Mathematical Society, Providence, R.I., 1978.
- [7] M. Reed and B. Simon. *Methods of modern mathematical physics. IV. Analysis of operators*. Academic Press [Harcourt Brace Jovanovich, Publishers], New York-London, 1978.
- [8] N. Fenichel. *Geometric singular perturbation theory for ordinary differential equations*. J. Differential Equations **31** (1979), 53–98.
- [9] B. Fiedler and K. Mischaikow. *Dynamics of bifurcations for variational problems with $O(3)$ equivariance: a Conley index approach*. Arch. Rational Mech. Anal. **119** (1992), 145–196.
- [10] B. Fiedler and A. Scheel. *Spatio-Temporal Dynamics of Reaction-Diffusion Patterns*. In Trends in Nonlinear Analysis, Springer-Verlag, Berlin (2003), 23–153.
- [11] B. Fiedler, A. Scheel, and M.I. Vishik. *Large Patterns of Elliptic Systems in Infinite Cylinders*. J. Math. Pures Appl. **77** (1998), 879–907.

- [12] G. Fusco and J.K. Hale. *Slow-motion manifolds, dormant instability, and singular perturbations*. J. Dynam. Differential Equations **1** (1989), 75–94.
- [13] K.P. Hadeler and F. Rothe. *Travelling fronts in nonlinear diffusion equations*. J. Math. Biol. **2** (1975), 251–263.
- [14] J. K. Hale. Asymptotic behavior of dissipative systems. *Mathematical Surveys and Monographs*, **25**. American Mathematical Society, Providence, RI, 1988.
- [15] G. Iooss and A. Mielke. *Bifurcating time-periodic solutions of Navier-Stokes equations in infinite cylinders*. J. Nonlinear Sci. **1** (1991), 107–146.
- [16] K. Kirchgässner. *Wave solutions of reversible systems and applications*. J. Differential Equations **45** (1982), 113–127.
- [17] B. Sandstede and A. Scheel. *On the stability of periodic travelling waves with large spatial period*. J. Diff. Eqns. **172** (2001), 134–188.
- [18] B. Sandstede and A. Scheel. *Absolute and convective instabilities of waves on unbounded and large bounded domains*. Phys. D **145** (2000), 233–277.
- [19] B. Sandstede and A. Scheel. *On the structure of spectra of modulated travelling waves*. Math. Nachr. **232** (2001), 39–93.
- [20] B. Sandstede and A. Scheel. *Essential instabilities of fronts: bifurcation and bifurcation failure*. Dyn. Syst. **16** (2001), 1–28.
- [21] B. Sandstede and A. Scheel. *Spectral stability of modulated travelling waves bifurcating near essential instabilities*. Proc. Roy. Soc. Edinburgh Sect. A **130** (2000), 419–448.
- [22] A. Scheel. *Existence of fast traveling waves for some parabolic equations: a dynamical systems approach*. J. Dynam. Differential Equations **8** (1996), 469–547.
- [23] W. van Saarloos. *Front propagation into unstable states*. Phys. Rep. **386** (2003), 29–222.
- [24] H. Weinberger. *On spreading speeds and traveling waves for growth and migration models in a periodic habitat*. J. Math. Biol. **45** (2002), 511–548 and J. Math. Biol. **46** (2003), 190.